

Preserving Causality in Time Domain Integral Equation-Based Methods

Loreto, Fabrizio ; Romano, Daniele ; Antonini, Giulio ; Stumpf, Martin; Lager, Ioan E.; Vandenbosch, Guy A.E.

DOI

[10.23919/EuMC50147.2022.9784233](https://doi.org/10.23919/EuMC50147.2022.9784233)

Publication date

2022

Document Version

Final published version

Published in

Proceedings of the 51st European Microwave Conference

Citation (APA)

Loreto, F., Romano, D., Antonini, G., Stumpf, M., Lager, I. E., & Vandenbosch, G. A. E. (2022). Preserving Causality in Time Domain Integral Equation-Based Methods. In *Proceedings of the 51st European Microwave Conference* (pp. 474-477). Article 9784233 IEEE.
<https://doi.org/10.23919/EuMC50147.2022.9784233>

Important note

To cite this publication, please use the final published version (if applicable).
Please check the document version above.

Copyright

Other than for strictly personal use, it is not permitted to download, forward or distribute the text or part of it, without the consent of the author(s) and/or copyright holder(s), unless the work is under an open content license such as Creative Commons.

Takedown policy

Please contact us and provide details if you believe this document breaches copyrights.
We will remove access to the work immediately and investigate your claim.

Green Open Access added to TU Delft Institutional Repository

'You share, we take care!' - Taverne project

<https://www.openaccess.nl/en/you-share-we-take-care>

Otherwise as indicated in the copyright section: the publisher is the copyright holder of this work and the author uses the Dutch legislation to make this work public.

Preserving Causality in Time Domain Integral Equation-Based Methods

Fabrizio Loreto[#], Daniele Romano[#], Giulio Antonini[#], Martin Stumpf^{*}, Ioan E. Lager[†], Guy A.E. Vandenbosch[^]

[#]UAq EMC Laboratory, University of L'Aquila, Italy

^{*}Department of Radioelectronics, Brno University of Technology, Czech Republic

[†]Delft University of Technology, The Netherlands

[^]Department of Electrical Engineering, Katholieke Universiteit Leuven, Belgium

fabrizio.loreto@graduate.univaq.it, {daniele.romano, giulio.antonini}@univaq.it, martin.stumpf@centrum.cz, i.e.lager@tudelft.nl, guy.vandenbosch@kuleuven.be

Abstract— The critical relevance of ensuring the excitation's causality in electromagnetic (EM) simulations is exploited by the computation of strictly causal time domain interaction integrals as they occur in the partial element equivalent circuit (PEEC) method. Under the hypothesis of thin, almost zero thickness objects, the presented formulas represent analytical impulse responses and, as such, are used within convolutions in the framework of the time domain PEEC solver. The proposed approach is compared with other standard approaches and clearly behaves better than frequency-domain methods in accurately catching the propagation delay and, thus, preserving the causality. Further, improved stability is observed compared to marching-on-in-time methods.

Keywords— Causality, time domain integral equation methods, partial element equivalent circuit (PEEC) method.

I. INTRODUCTION

Time domain integral equation (TDIE) methods are an attractive alternative to the finite difference/element methods for analyzing transient electromagnetic (EM) phenomena [1], [2], [3], [4]. TDIE methods are typically solved by marching-on-in-time (MOT) schemes. It is well known that MOT schemes suffer from late-time instabilities [3], [5]. Over the years, many papers have investigated diverse smooth time basis functions to interpolate the value of the retarded electromagnetic quantities between the past solution samples. In this regard, it is clear that the treatment of propagation delay is important both for the accuracy of the result and for ensuring the stability of the MOT scheme. Another physical feature, strictly related to the propagation delay which should be preserved in the modeling process, is causality.

Among the integral-equation based techniques, the PEEC method has gained popularity thanks to its ability to represent electromagnetic (EM) phenomena in terms of equivalent circuits [6]. It is based on the volume equivalence principle and, differently from the method of moments (MoM) [7], it keeps currents and charges separate. The electric field integral equation (EFIE) and the continuity equation are solved upon a pertinent expansion of the unknowns and applying the Galerkin's projection method. If propagation delays are neglected, standard RLC circuits are obtained

which are modeled in the time domain by a system of ordinary differential equations (ODEs) by enforcing Kirchhoff principles. If the propagation delays are taken into account, they can be approximated by using the center to center distance between the spatial support of basis functions. In this case, a set of delayed differential equations of the neutral type (NDDEs) are obtained [8] which are solved by means of MOT schemes. This approach has been used for a long time and it is however affected by instability problems. More recently, the numerical inversion of Laplace transform (NILT) has been proposed as a valid alternative to the MOT approach [9]. NILT-based solution of PEEC models exhibits improved stability and better accuracy although at the cost of a greater computational load.

Recently, a novel analytical approach for computing retarded coefficients of potential of a PEEC model based on the Cagniard-de Hoop (CdH) technique [10] has been presented for identical coplanar rectangular patches [11]. The aim of this work is to extend the analytical solution to the case of non-identical coplanar rectangular patches and demonstrate that it can be derived analytically in the time domain (TD) in terms of elementary functions only. Then, since the same analytical formulas can be adopted also for the interaction integrals describing the magnetic field impulse response, some preliminary results obtained by using the analytical impulse responses along with convolution schemes are presented and compared with other, well-established techniques.

II. CAUSALITY OF LTI DISTRIBUTED SYSTEMS

Causality is the physical property of a system expressing that a response cannot precede the cause that produces it. It should be strictly preserved by numerical time domain models.

Let us consider a time-invariant electromagnetic system¹ with input and output denoted, respectively, by the n -element vectors $\mathbf{x}(t)$ and $\mathbf{w}(t)$. Let us denote with $\mathbf{h}(t)$ the system impulse response matrix with each element $h_{ij}(t)$ being the response at port i when an ideal impulse (Dirac's delta) is

¹The time-invariance property identifies those systems that do not change their behavior with time. If $\mathbf{w}(t)$ is the output excited by input $\mathbf{x}(t)$, then $\mathbf{w}(t - \tau)$ is the output for the delayed input $\mathbf{x}(t - \tau)$.

applied at port j , with all other inputs set to zero. The definition of causality for distributed systems that are affected by the finite value of speed of the electromagnetic field requires the following condition to be satisfied:

$$h_{ij}(t) = 0, \quad t < \tau_{ij}, \quad \tau_{ij} > 0, \quad \forall i, j. \quad (1)$$

where τ_{ij} represent the time delay between the input j and the output i .

III. INTERACTION INTEGRALS IN THE PEEC METHOD

The Partial Elements Equivalent Circuit (PEEC) method is an integral equation-based technique able to provide a circuit representation of the EM problem. Since it is based on the volume equivalence principle, electric current densities flowing in conducting volumes, polarization currents flowing in dielectric volumes and charges located on the surface of conductors are assumed to radiate in the background medium (i.e. the free space). Hence, the free space Green's function is adopted. Upon a pertinent discretization of the geometry of interest in elementary volumes and patches, two types of interactions have to be considered: a) magnetic field interactions between elementary volumes where electric currents flow; b) electric field interactions between elementary surfaces where electric charges are assumed to be located. The magnetic field interactions are described by the partial inductances [6]. If we consider two elementary volumes $\mathcal{V}_m, \mathcal{V}_n$, the mutual partial inductance in the Laplace domain is defined as:

$$L_{p_{mn}}(s) = \frac{\mu_0}{4\pi} \int_{\mathbf{r} \in \mathcal{V}_m} \int_{\mathbf{r}' \in \mathcal{V}_n} \mathbf{f}_m(\mathbf{r}) \cdot \mathbf{f}_n(\mathbf{r}') g(\mathbf{r} - \mathbf{r}', s) dV dV' \quad (2)$$

where \mathbf{r} and \mathbf{r}' are the observation and source points located in volumes \mathcal{V}_m and \mathcal{V}_n , respectively, \mathbf{f}_m and \mathbf{f}_n are the vector basis functions and

$$g(\mathbf{r} - \mathbf{r}', s) = \frac{\exp[-s|\mathbf{r} - \mathbf{r}'|/c_0]}{4\pi|\mathbf{r} - \mathbf{r}'|} \quad (3)$$

is the Green's function pertaining to a homogeneous, isotropic and loss-free medium described by its (scalar and real-valued) electric permittivity ϵ_0 and magnetic permeability μ_0 with the corresponding EM wave speed $c_0 = (\epsilon_0\mu_0)^{-1/2} > 0$ in the background medium.

The electric field interactions are described by the coefficients of potential [6]. If we consider two surface patches, the mutual coefficient of potential in the Laplace domain reads:

$$P_{mn}(s) = \frac{1}{4\pi\epsilon_0} \frac{1}{\mathcal{A}_m \mathcal{A}_n} \int_{\mathbf{r} \in \mathcal{A}_m} \int_{\mathbf{r}' \in \mathcal{A}_n} g(\mathbf{r} - \mathbf{r}', s) d\mathcal{S} d\mathcal{S}' \quad (4)$$

where \mathcal{A}_m and \mathcal{A}_n are the surfaces of patches m and n and constant basis functions have been assumed. Typically, integrals (2), (4) are computed in the frequency-domain ($s = j\omega$) through a numerical Gaussian adaptive scheme, where the integration order is automatically set depending on the distance between the spatial supports of the two basis functions m and n , higher when the volumes are close, and lower when they are far away. The inverse fast Fourier transform (IFFT) algorithm

can be used to restore the transient partial inductance, but a very large amount of samples is typically required for an adequate result free of aberrations. This is not compatible with the computation of a large number of partial elements. In the case of coplanar identical rectangular patches, analytical expressions for the time domain counterparts of (2) and (4), $L_{p_{mn}}(t), P_{mn}(t)$, exist [11]. In the next section, this result is extended to coplanar, but not identical, rectangular patches.

IV. TIME DOMAIN ANALYTICAL SOLUTION

We assume to start from a hexahedral mesh of the system under analysis. In the following, we restrict our analysis to thin objects so that the same type of integral hold for both the interaction integrals (2) and (4), leading to $L_{p_{mn}}(t)$ and $P_{mn}(t)$, apart from a scaling factor. Hence, we shall limit ourselves in this work to the interaction of two *parallel* rectangular surface elements of different sizes lying on the same plane (see Fig. 1) which are the spatial support of charges and currents.

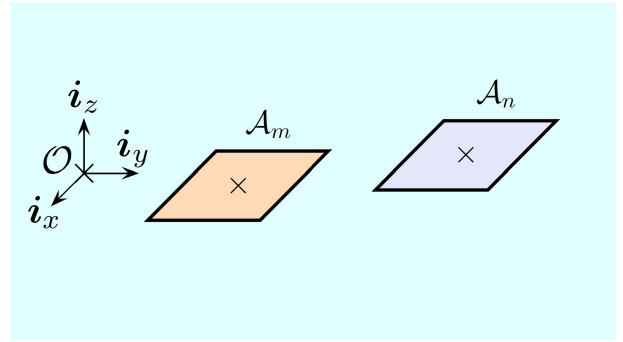


Fig. 1. Two rectangular parallel patches.

To localize the position in the problem configuration, we employ coordinates $\{x, y, z\}$ with respect to an orthogonal Cartesian reference frame with the origin \mathcal{O} and the standard basis $\{i_x, i_y, i_z\}$. Consequently, the position vector is $\mathbf{r} = x\mathbf{i}_x + y\mathbf{i}_y + z\mathbf{i}_z$. The time coordinate is denoted by t .

For parallel patches with different size, the surface retarded interaction integral in (4) can be expressed in the Laplace-domain through a double 2-D integral:

$$I_{mn}(s) = \int_{\mathbf{r} \in \mathcal{A}_m} dS \int_{\mathbf{r}' \in \mathcal{A}_n} g(\mathbf{r} - \mathbf{r}', s) dS' \quad (5)$$

where, if (x_i, y_i) are the coordinates of the basis-function support center, $\mathcal{A}_m = \{-\Delta_x^m/2 < x - x_m < \Delta_x^m/2, -\Delta_y^m/2 < y - y_m < \Delta_y^m/2, z = 0\}$ and $\mathcal{A}_n = \{-\Delta_x^n/2 < x - x_n < \Delta_x^n/2, -\Delta_y^n/2 < y - y_n < \Delta_y^n/2, z = 0\}$, with $\Delta_x^{m,n} > 0$ and $\Delta_y^{m,n} > 0$ represent the widths of the patches m and n along the x and y axes of the cartesian system of coordinates. Furthermore, s is the real-valued and positive Laplace-transform parameter [12], $\mathcal{S}_{m,n} = \Delta_x^{m,n} \Delta_y^{m,n}$ are the surface areas of domains $\mathcal{A}_{m,n}$, respectively.

Pursuing the approach introduced in Ref. [11], the TD counterpart of Eq. (5) can be derived. In this way, an extension of [11, Eq. (7)] pertaining to the actual problem definition (see Fig. 1) can be expressed as:

$$\begin{aligned}
I_{mn}(t) = & \\
& \left[I(x_m - x_n + \Delta_x^{mn+}, y_m - y_n + \Delta_y^{mn+}, t) \right. \\
& - I(x_m - x_n + \Delta_x^{mn+}, y_m - y_n + \Delta_y^{mn-}, t) \\
& - I(x_m - x_n + \Delta_x^{mn+}, y_m - y_n - \Delta_y^{mn-}, t) \\
& + I(x_m - x_n + \Delta_x^{mn+}, y_m - y_n - \Delta_y^{mn+}, t) \\
& - I(x_m - x_n + \Delta_x^{mn-}, y_m - y_n + \Delta_y^{mn+}, t) \\
& - I(x_m - x_n - \Delta_x^{mn-}, y_m - y_n + \Delta_y^{mn+}, t) \\
& + I(x_m - x_n + \Delta_x^{mn-}, y_m - y_n + \Delta_y^{mn-}, t) \\
& + I(x_m - x_n + \Delta_x^{mn-}, y_m - y_n - \Delta_y^{mn-}, t) \\
& + I(x_m - x_n - \Delta_x^{mn-}, y_m - y_n + \Delta_y^{mn-}, t) \\
& + I(x_m - x_n - \Delta_x^{mn-}, y_m - y_n - \Delta_y^{mn-}, t) \\
& - I(x_m - x_n + \Delta_x^{mn-}, y_m - y_n - \Delta_y^{mn+}, t) \\
& - I(x_m - x_n - \Delta_x^{mn-}, y_m - y_n - \Delta_y^{mn+}, t) \\
& + I(x_m - x_n - \Delta_x^{mn+}, y_m - y_n + \Delta_y^{mn+}, t) \\
& - I(x_m - x_n - \Delta_x^{mn+}, y_m - y_n + \Delta_y^{mn-}, t) \\
& - I(x_m - x_n - \Delta_x^{mn+}, y_m - y_n - \Delta_y^{mn-}, t) \\
& + I(x_m - x_n - \Delta_x^{mn+}, y_m - y_n - \Delta_y^{mn+}, t) \left. \right] \quad (6)
\end{aligned}$$

where:

$$\Delta_{x,y}^{mn\pm} = (\Delta_{x,y}^m \pm \Delta_{x,y}^n)/2 \quad (7)$$

and $I(x, y, t)$ is defined by [11, Eq. (21)]. Then, the TD coefficient of potential is obtained from (6) as

$$P_{mn}(t) = (\varepsilon_0 \mathcal{S}_m \mathcal{S}_n)^{-1} I_{mn}(t) \quad (8)$$

Similarly, the TD mutual partial inductance for two thin volumes can be deduced from (6) as follows:

$$L_{p_{mn}}(t) = \frac{\mu_0 \mathcal{T}_m \mathcal{T}_n}{4\pi \mathcal{S}_{cm} \mathcal{S}_{cn}} I_{mn}(t) = \frac{\mu_0}{4\pi \mathcal{W}_m \mathcal{W}_n} I_{mn}(t) \quad (9)$$

where $\mathcal{S}_{cm} = \mathcal{W}_m \mathcal{T}_m$, $\mathcal{S}_{cn} = \mathcal{W}_n \mathcal{T}_n$, are the cross sections of the two volumes and an orthogonal mesh resulting in parallelepipeds is assumed. $\mathcal{W}_{m,n}$ coincides with Δ_y^{mn} or Δ_x^{mn} depending whether the current is directed along the x - or the y -axis.

Figure 2 shows the normalized mutual potential coefficients, computed using (6) and (8), between two square patches of width $\mathcal{W}_1 = \mathcal{W}_2 = 1$ mm placed at different minimum distance R_m ranging from 0 up 4.2 mm. It is evident that the propagation delay effect is perfectly reproduced by the computed impulse responses, hence the causality is strictly guaranteed as the response is zero for $t < t_{min} = R_{min}/c_0$, where R_{min} is the minimum distance between patches m and n . Furthermore, the two patches interact up to $t_{max} = R_{max}/c_0$ where R_{max} is the maximum distance between patches m and n , hence the interaction integral $I_{mn}(t)$ is strictly time-limited. The transient partial inductances and coefficients of potential are then implemented into a time domain solver and convolved with time derivative of currents and charges. The convolution integrals are computed through the segment fast convolution scheme [13].

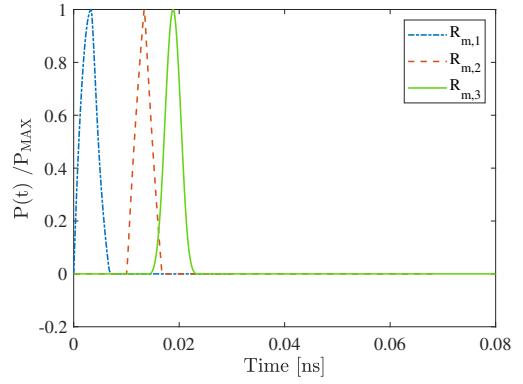


Fig. 2. $P(t)$ evaluated at minimum distances: $R_{m,1} = 0$ mm (touching patches), $R_{m,2} = 3$ mm, $R_{m,3} = 4.2$ mm.

V. NUMERICAL RESULTS

The previous theoretical concepts are now exemplified via a simple, yet illustrative configuration consisting of two nearby-located, linear dipoles, one in the transmitting mode and one in the receiving mode. We assume the dipoles to be very thin, in order to use the analytical formulas for the interaction integrals of both partial inductances (2) and coefficients of potential (4). Referring to Fig. 3, the geometric details are summarized in Table 1.

Table 1. Dipoles geometric details.

arm length	$\ell = 5$ cm
arm width	$w = 1$ mm
distance between dipoles	$d = 20$ cm
gap length	$g = 5$ mm
thickness	$t \approx 0$ mm

Two dual meshes are adopted to model the flow of currents and the distribution of charges [6]. Generally, also in this simple configuration, the mesh that gives rise to potential coefficients require the coexistence of different sizes patches; hence the expression (5) is strictly necessary to describe the electric coupling between patches of different sizes.

The transmitting dipole is center-fed by a real voltage source having an internal impedance of 73Ω and the receiving dipole is center-closed over a 73Ω load. The transient voltage source is chosen so to have finite time temporal support [14]. It is described by

$$v_s(\nu, t) = V_0 N(\nu) 2\nu \left(1 - \frac{t}{t_r}\right) \left(\frac{t}{t_r}\right)^{\nu-1} \left(2 - \frac{t}{t_r}\right)^{\nu-1} \quad (10)$$

with $N = \nu^{-1} 2^{-\nu} (\nu - 1)^{1-\nu} (2\nu - 1)^{\nu-1/2}$. An example with amplitude $V_0 = 0.59$ V, $\nu = 4$, rise time $t_r = 3.7$ ns is illustrated in Fig. 4a. The analytical impulse responses for the magnetic and electric field interactions as given in (8) and (9) obtained by the Cagniard-deHoop technique are used in a time domain convolution-based solver, leading to the time domain behaviour of currents, charges and potentials of the dipoles. As stated before, the segment fast convolution has been adopted [13] to perform the convolution integrals. The convolution-based results (CdH-SFC) are compared with those obtained through several

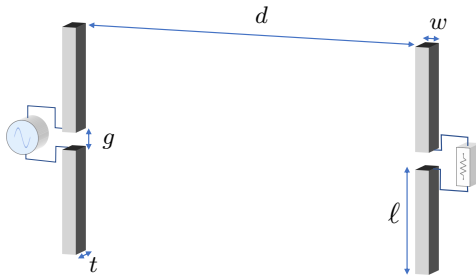


Fig. 3. Dipole antennas.

techniques: a frequency-domain solver involving the fast Fourier transform (FFT) of the time domain partial elements coefficients (CdH-IFFT), a frequency-domain solver involving the partial elements computed through the center to center approximation (CC-IFFT) and a marching-on-in-time solver that adopts triangular temporal basis functions (TBF-MOT) for the partial elements. For the frequency-domain solvers, the time domain response is restored by the inverse fast fourier transform scheme (IFFT). The voltage $v_2(t)$ across the load of the receiving dipole is shown in Fig. (4a). A satisfactory agreement is observed in general among all the methods, but it is evident from Fig. (4b) that causality is better reproduced by the time domain convolution-based solver compared to the frequency-domain solvers which suffer from the truncation of the spectrum. Based on our experience, MOT techniques are frequently very sensitive to the choice of time step and the method of integration. Consequently, the corresponding MOT computational schemes may become unstable. The proposed approach is found to be always stable in our tests. This confirms that accuracy, causality and stability are strictly related.

VI. CONCLUSION

In this work, the causality of interaction integrals occurring in time domain integral equation based methods has been considered. In particular, strictly causal time domain interaction integrals between coplanar patches as they occur in the partial element equivalent circuit (PEEC) method are proposed under the hypothesis of thin objects. The comparison with more standard techniques on a antenna test case shows that the proposed approach outperforms frequency-domain methods in reproducing causality. Preliminary results also exhibit improved stability properties which will be investigated in the future.

REFERENCES

- [1] R. G. Martin, A. Salinas, and A. R. Bretones, "Time-domain integral equation methods for transient analysis," vol. 34, no. 3, pp. 15–22, 1992.
- [2] G. Manara, A. Monorchio, and R. Reggiannini, "A space-time discretization criterion for a stable time-marching solution of the electric field integral equation," *IEEE Transactions on Antennas and Propagation*, vol. 45, no. 3, pp. 527–532, Mar 1997.
- [3] S. M. Rao, *Time Domain Electromagnetics*. London: Academic Press, 1999.
- [4] A. Al-Jarro, M. A. Salem, H. Bagci, T. M. Benson, P. Sewell, and A. Vukovic, "Explicit solution of the time domain volume integral equation using a stable predictor-corrector scheme," *IEEE Transactions on Antennas and Propagation*, vol. 60, no. 11, pp. 5203–5214, Nov 2012.
- [5] W. L. G. Xiao, X. Tian and J. Fang, "Impulse responses and the late time stability properties of time-domain integral equations," vol. 9, no. 7, pp. 603–610, Jan. 2015.
- [6] A. E. Ruehli, G. Antonini, and L. Jiang, *Circuit Oriented Electromagnetic Modeling Using the PEEC Techniques*. Wiley-IEEE Press, 2017.
- [7] R. F. Harrington, *Field Computation by Moment Methods*. Malabar: Krieger, 1982.
- [8] A. Bellen, N. Guglielmi, and A. Ruehli, "Methods for linear systems of circuit delay differential equations of neutral type," vol. 46, no. 1, pp. 212–216, Jan. 1999.
- [9] L. Lombardi, F. Loreto, F. Ferranti, A. Ruehli, M. S. Nakhla, Y. Tao, M. Parise, and G. Antonini, "Time-domain analysis of retarded partial element equivalent circuit models using numerical inversion of laplace transform," *IEEE Transactions on Electromagnetic Compatibility*, pp. 1–10, 2020.
- [10] A. T. De Hoop, "A modification of Cagniard's method for solving seismic pulse problems," *Applied Scientific Research*, vol. B, no. 8, pp. 349–356, 1960.
- [11] M. Štumpf, G. Antonini, and A. Ruehli, "Cagniard-DeHoop technique-based computation of retarded partial coefficients: The coplanar case," *IEEE Access*, vol. 8, pp. 148 989–148 996, 2020.
- [12] M. Stumpf, *Electromagnetic Reciprocity in Antenna Theory*. Wiley-IEEE Press, 2017.
- [13] P. Belforte, D. Spina, L. Lombardi, G. Antonini, and T. Dhaene, "Automated framework for time-domain piecewise-linear fitting method based on digital wave processing of S -parameters," *IEEE Transactions on Circuits and Systems I: Regular Papers*, vol. 67, no. 1, pp. 235–248, 2020.
- [14] I. E. Lager and S. L. van Berkel, "Finite temporal support pulses for EM excitation," *IEEE Antennas and Wireless Propagation Letters*, vol. 16, pp. 1659–1662, 2017.

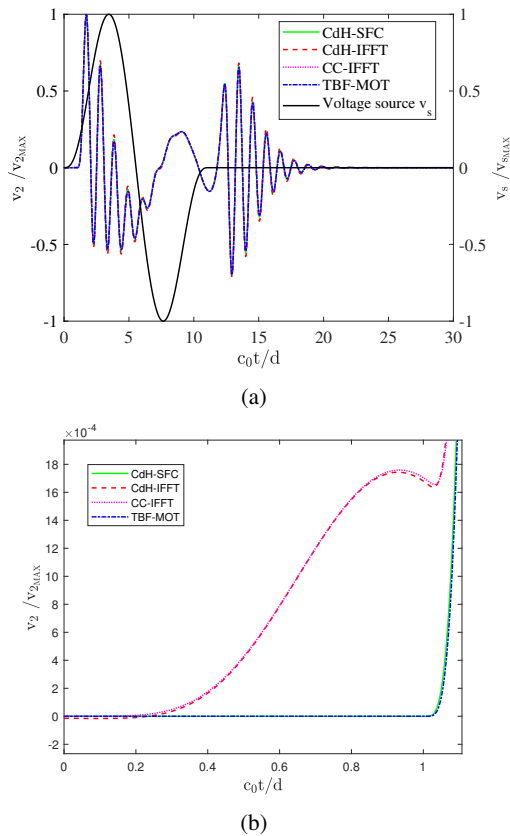


Fig. 4. Receiving dipole: (a) Voltage v_2 (the shape of the exciting pulse is provided for comparison). (b) Zoom-in of the voltage v_2 .